

BU-HEPP-06-01  
TRI-PP-02-01

# Strange-quark Current in the Nucleon from Lattice QCD

Randy Lewis

*Department of Physics, University of Regina, Regina SK, Canada S4S 0A2*

W. Wilcox

*Department of Physics, Baylor University, Waco TX 76798-7316, U.S.A.*

R.M. Woloshyn

*TRIUMF, 4004 Wesbrook Mall, Vancouver BC, Canada V6T 2A3*

Presented at the International Symposium on Electromagnetic Interactions in Nuclear and Hadron Physics, Osaka, Japan, 4th to 7th December, 2001.



# STRANGE-QUARK CURRENT IN THE NUCLEON FROM LATTICE QCD

RANDY LEWIS

*Department of Physics, University of Regina, Regina SK, Canada S4S 0A2*

W. WILCOX

*Department of Physics, Baylor University, Waco TX 76798-7316, U.S.A.*

R.M. WOLOSHYN

*TRIUMF, 4004 Wesbrook Mall, Vancouver BC, Canada V6T 2A3*

The contribution of the strange-quark current to the electromagnetic form factors of the nucleon is studied using lattice QCD. The strange current matrix elements from our lattice calculation are analyzed in two different ways, the differential method used in an earlier work by Wilcox and a cumulative method which sums over all current insertion times. The preliminary results of our simulation indicate the importance of high statistics, and that consistent results between the varying analysis methods can be achieved. Although this simulation does not yet yield a number that can be compared to experiment, several criteria useful in assessing the robustness of a signal extracted from a noisy background are presented.

## 1 Introduction

An important theme of contemporary Hadron Physics is the role of nonvalence degrees of freedom. In particular, the contribution of strange quarks to a variety of nucleon properties has been studied.<sup>1</sup> For nucleon form factors the contribution of the strange-quark current can be extracted using information obtained from parity violation in polarized electron scattering.<sup>2</sup> A number of experimental results have been reported<sup>3,4</sup> and new measurements are planned. As well, there are numerous calculations using a number of different approaches.<sup>2</sup>

In this work we focus on the calculation of the strange-quark current loop using lattice QCD. Calculations of these so-called disconnected current insertions have been reported previously.<sup>5,6,7</sup> However, these calculations differ in the method used to analyze the results of their lattice simulations and also differ in their conclusions. Wilcox<sup>5</sup> used a differential method to analyze the time dependence of the three-point function and no signal for the strange current was found. On the other hand, Dong and co-workers<sup>6,7</sup> used a summation of the current insertion over lattice times which requires a further identification and fitting of a linear time dependence. They claim to see a

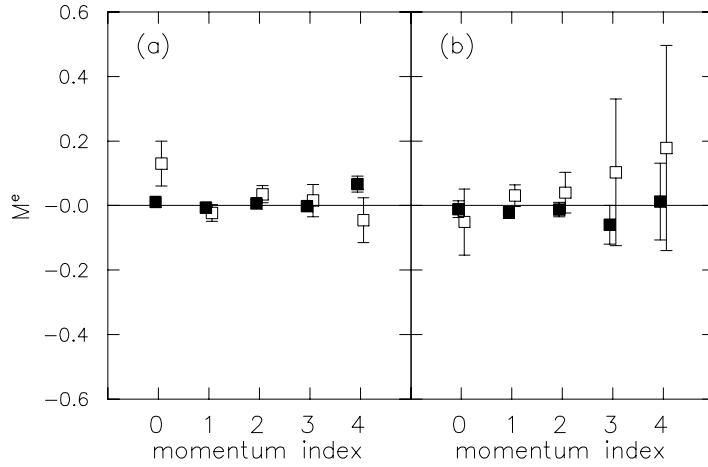


Figure 1. Comparison of the electric matrix element calculated with the differential method for samples of 100 configurations (open symbols) and 1050 configurations (filled symbols). (a) Average of times 10 to 12. (b) Average of times 15 to 17.

definite signal for the strangeness form factors.

We present preliminary results from a lattice QCD simulation of the strange-quark current loop using a Monte-Carlo sample of gauge field configurations about ten times larger than in previous studies. Both differential and cumulative time analyses are carried out on the simulation data. Comparisons of results obtained from a 100 configuration subsample (the same size used in previous work<sup>5,6,7</sup>) with results from the full data set show quite clearly how large fluctuations, that could be interpreted as a signal in low-statistics data, disappear with improved statistics. Using our complete data set consistency between different analysis methods is achieved. By comparing different analysis methods and results using different sized gauge field samples, criteria for assessing the robustness of a strange quark current signal are presented. Using these criteria, no compelling signal for the strange quark current is observed.

## 2 Lattice Calculations

The standard methods of the path integral formulation of lattice QCD in Euclidean space are used. The Wilson action is used for both quark and gluon fields. We need two and three-point functions which describe, respectively, the

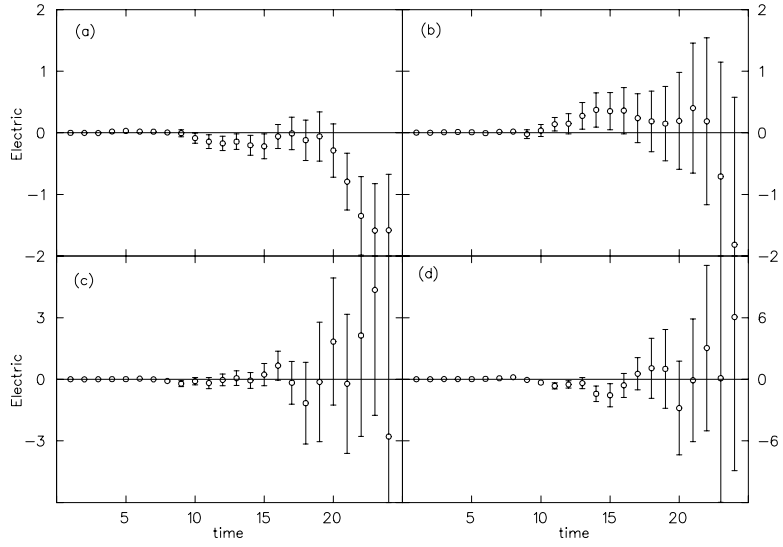


Figure 2. Electric matrix element using the cumulative method for a sample of 100 configurations. The plots correspond to momentum transfer (a)  $(1,0,0)$ , (b)  $(1,1,0)$ , (c)  $(1,1,1)$ , (d)  $(2,0,0)$ .

propagation of nucleon states as a function of Euclidean lattice time and the strange quark current in the presence of a nucleon. The two-point function  $G^{(2)}(t; \vec{q})$  correlates the excitation of a nucleon state with momentum  $\vec{q}$  at some initial time (called 0) and its annihilation at time  $t$ . For large Euclidean time  $t$  this quantity decreases exponentially like  $e^{-E_q t}$ .

To calculate the three-point function  $G^{(3)}(t, t'; \vec{q})$  an insertion of the strange-quark vector current is made at time  $t'$ . Since there are no strange valence quarks in the nucleon this insertion amounts to a correlation of a strange-quark current loop with the nucleon two-point function. The strange-quark current loop is calculated using a so-called noisy estimator with  $Z_2$  noise<sup>8,9</sup>. The noise and perturbative subtraction methods employed here are the same as those of Wilcox<sup>5</sup> except that 60 noises are used instead of 30.

The three-point function also has an exponential time dependence but is more complicated due to the presence of two times. It can be shown that the exponential time factors can be cancelled by taking the ratio

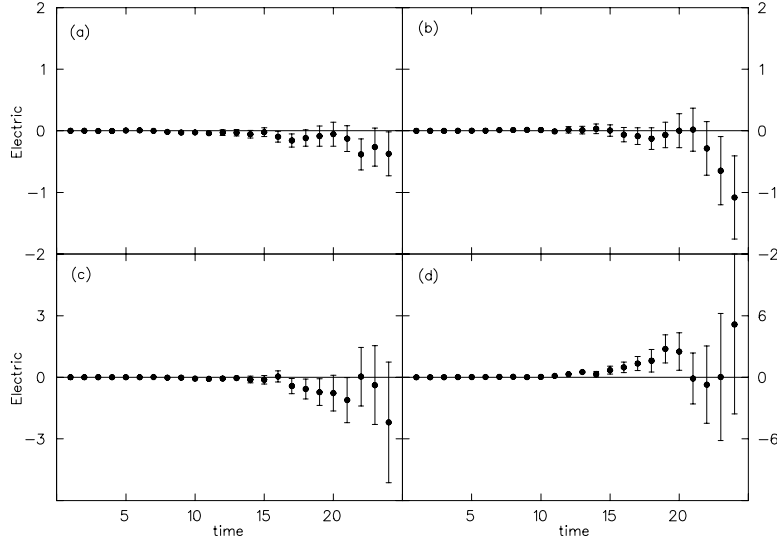


Figure 3. Electric matrix element using the cumulative method for a sample of 1050 configurations. The plots correspond to momentum transfer (a) (1,0,0), (b) (1,1,0), (c) (1,1,1), (d) (2,0,0).

$$R(t, t'; \vec{q}) = \frac{G^{(3)}(t, t'; \vec{q})G^{(2)}(t'; 0)}{G^{(2)}(t; 0)G^{(2)}(t'; \vec{q})}. \quad (1)$$

It is these ratios  $R$  that are analyzed to get the final results.

Note that in writing the two and three-point functions, labels associated with the Dirac indices of the nucleon fields and the Lorentz index of the current have been suppressed. Also in writing Eq. (1) the necessary spin sums and projections are not shown, the expression is given schematically to show the time dependence of the various factors. The detailed calculations follow previous work.<sup>5,6,7</sup>

The ratio  $R$  is usually summed in order to try to improve the signal. The differential method uses a difference of  $R(t, t'; \vec{q})$  on neighbouring time slices. It can be shown<sup>5</sup> that the quantity  $M(\bar{t}, \vec{q})$  given by

$$M(\bar{t}, \vec{q}) = \sum_{t'=1}^{t+1} (R(t, t'; \vec{q}) - R(t-1, t'; \vec{q})) \quad (2)$$

is the current matrix element of interest.

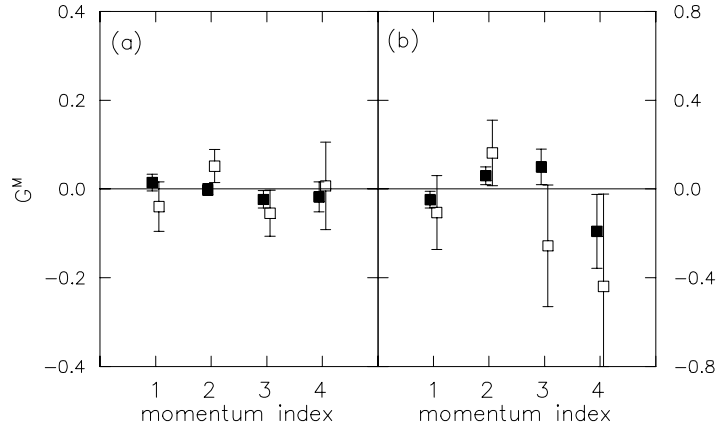


Figure 4. Comparison of the magnetic matrix element calculated with the differential method for samples of 100 configurations (open symbols) and 1050 configurations (filled symbols) using  $\kappa = 0.152$  for the valence quark. (a) Average of times 10 to 12. (b) Average of times 15 to 17.

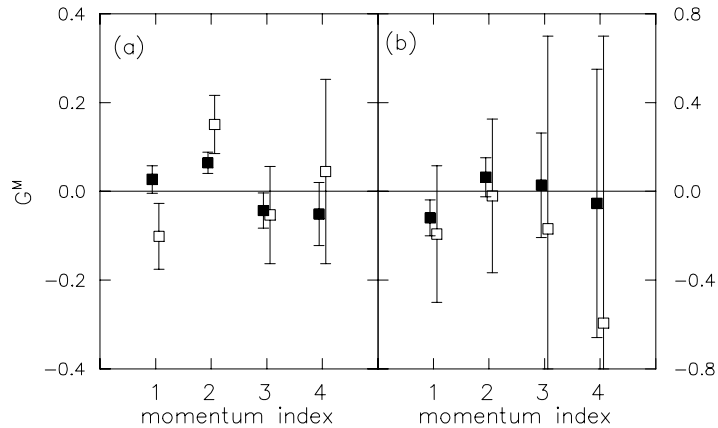


Figure 5. Comparison of the magnetic matrix element calculated with the differential method for samples of 100 configurations (open symbols) and 1050 configurations (filled symbols) using  $\kappa = 0.154$  for the valence quark. (a) Average of times 10 to 12. (b) Average of times 15 to 17.

An alternative is to simply sum  $R$  and then fit to a linear time dependence

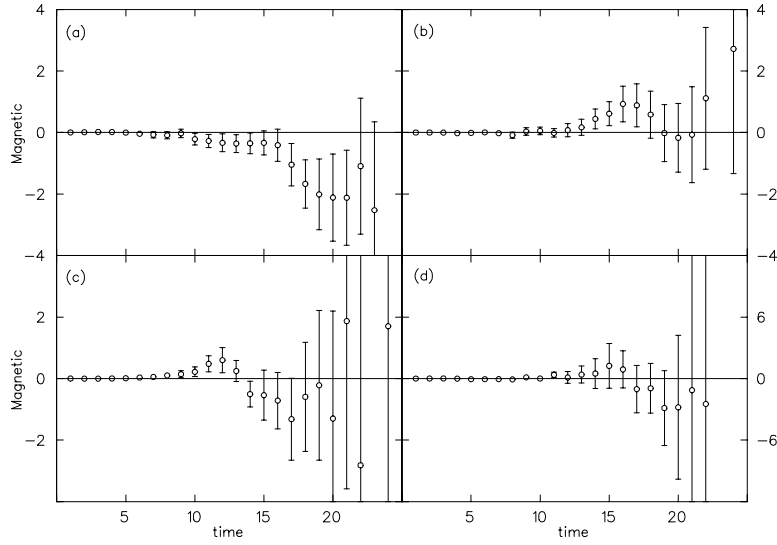


Figure 6. Magnetic matrix element using the cumulative method for a sample of 100 configurations with  $\kappa = 0.152$  valence quark. The plots correspond to momentum transfer (a)  $(1,0,0)$ , (b)  $(1,1,0)$ , (c)  $(1,1,1)$ , (d)  $(2,0,0)$ .

to get the matrix element. We use

$$S(t, \vec{q}) = \sum_{t'=1}^{t'=t} R(t, t'; \vec{q}), \quad (3)$$

$$\rightarrow \text{constant} + tM(t, \vec{q}). \quad (4)$$

Summing current insertions up to  $t' = t$  follows the suggestion of Viehoff *et al.*<sup>10</sup> and helps to reduce the statistical noise. Dong and co-workers<sup>6,7</sup> actually use a different upper limit ( $t' = t_{fixed}, t_{fixed} > t$ ).

### 3 Results

Calculations were carried out in quenched approximation at gauge field coupling of  $\beta = 6.0$ . The lattice size was  $20^3 \times 32$ . A total of 1050 gauge field configurations were generated using a pseudo-heat bath algorithm. Two thousand sweeps were used between saved configurations.

Since quenched lattice QCD does not provide a perfect description of hadrons, there is some ambiguity in fixing the parameters (overall scale and

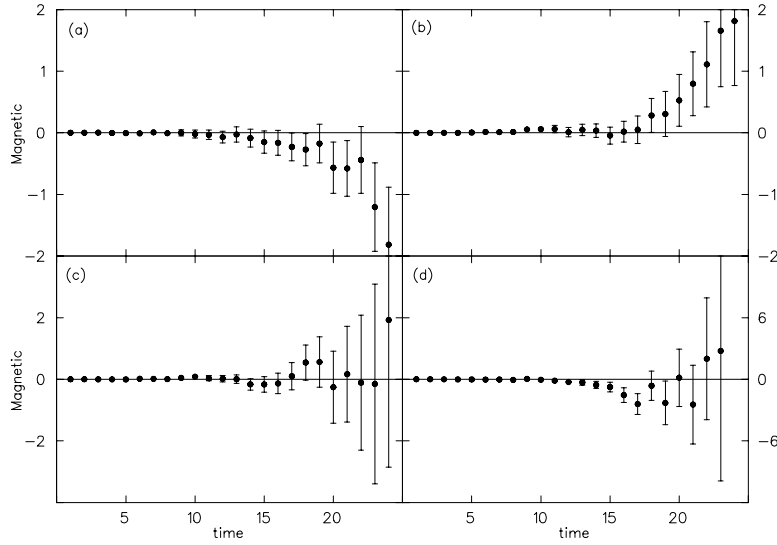


Figure 7. Magnetic matrix element using the cumulative method for a sample of 1050 configurations with  $\kappa = 0.152$  valence quark. The plots correspond to momentum transfer (a)  $(1,0,0)$ , (b)  $(1,1,0)$ , (c)  $(1,1,1)$ , (d)  $(2,0,0)$ .

quark masses) in the calculations. In this work we use 0.152 as the hopping parameter for the strange quark. Using  $a^{-1} = 2\text{GeV}$  and the  $\phi$ -meson to fix the strange quark mass would suggest a hopping parameter closer to  $\kappa_s = 0.153$ . On the other hand, using the scale of Dong and co-workers<sup>6,7</sup>  $a^{-1} = 1.74\text{GeV}$  gives  $\kappa_s$  smaller than 0.152.

Results for electric matrix element with valence quark  $\kappa_v = 0.152$  calculated using the differential method Eq. (2) are shown in Fig. (1), averaging over two different time windows. The 100 configuration sample results are consistent with those obtained by Wilcox<sup>5</sup>. No signal is seen when the gauge field sample size is increased to 1050. The summed ratio Eq. (3) is shown in Fig. (2) and (3) as a function of the nucleon sink time for different momentum transfers. It shows oscillations characteristic of lattice correlation function ratios<sup>11</sup>. The magnitude of these oscillations decreases slowly as the configuration sample size is increased.

Results for the magnetic matrix element for different valence quark masses calculated using the differential method are plotted in Fig. (4) and (5). As in the electric case the results are consistent with zero.

Finally, the summed ratios for the magnetic current are given in Fig. (6)

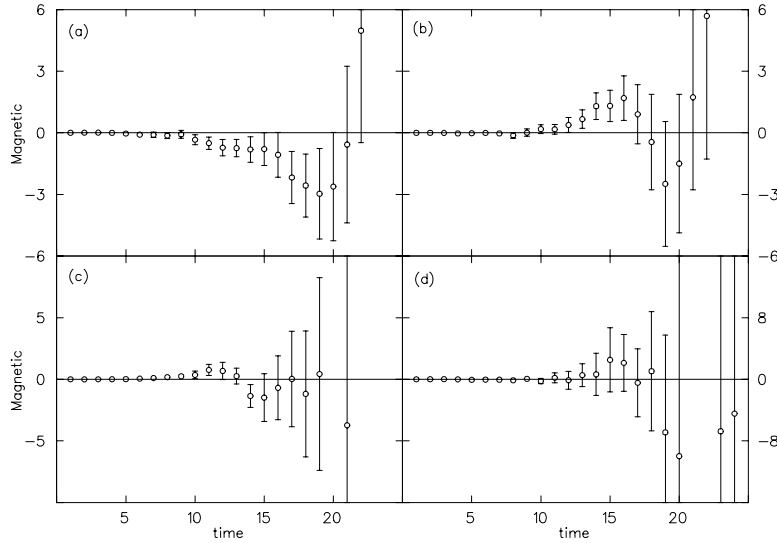


Figure 8. Magnetic matrix element using the cumulative method for a sample of 100 configurations with  $\kappa = 0.154$  valence quark. The plots correspond to momentum transfer (a)  $(1,0,0)$ , (b)  $(1,1,0)$ , (c)  $(1,1,1)$ , (d)  $(2,0,0)$ .

to Fig. (9). Note that a kinematic factor (see Eq. (3) in Ref.<sup>6</sup>) of  $q/(E + M)$  has been removed. The results for 100 configurations, Fig. (6) and (8), should be compared to Fig. (1) of Dong *et al.*<sup>6</sup> and Fig. (2) of Mathur and Dong<sup>7</sup> where calculations with the same statistics are reported. Then, comparing with Fig. (7) and (9), one sees that the kind of oscillations in the time range 10 to 15 which Dong and co-workers<sup>6,7</sup> took to be their signal, have largely disappeared in the higher statistics results. Of course, fluctuations still persist at larger times but even higher statistics simulations will be necessary to establish if they go away or if indeed a strange quark current signal is hiding under them.

#### 4 Conclusions

To get an estimate of the strange-quark current matrix elements requires the extraction of a small signal in the presence of large statistical fluctuations. The results presented here suggest a number of useful criteria that should be met before one can claim a credible signal:

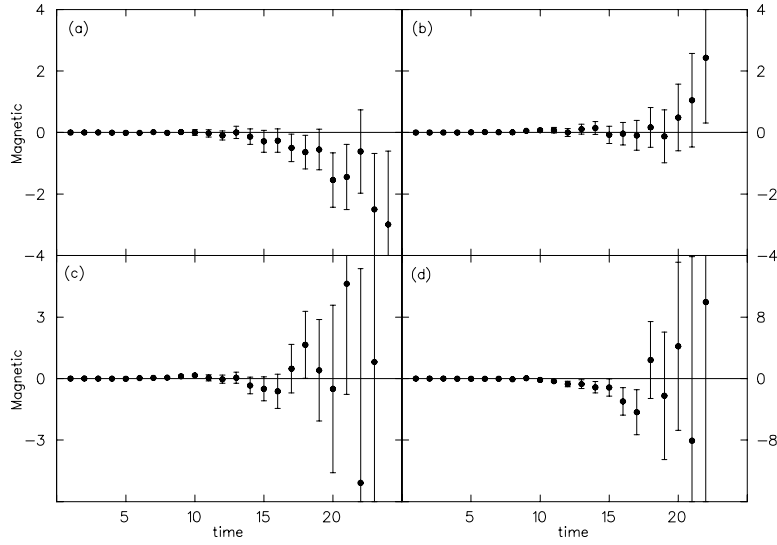


Figure 9. Magnetic matrix element using the cumulative method for a sample of 1050 configurations with  $\kappa = 0.154$  valence quark. The plots correspond to momentum transfer (a)  $(1,0,0)$ , (b)  $(1,1,0)$ , (c)  $(1,1,1)$ , (d)  $(2,0,0)$ .

- There should be consistency between different analysis methods.
- The signal should appear in the same lattice time region and its statistical significance should increase as the size of the Monte-Carlo sample of gauge fields is increased.
- The signal should appear in the same time window for different masses.

Not all of these criteria have been met at our present level of statistics. Work is continuing and it is hoped to have final results with an increased configuration sample size in the not too distant future.

### Acknowledgments

This work is supported in part by the National Science Foundation under grant 0070836 and in part by the Natural Sciences and Engineering Research Council of Canada. We thank N. Mathur for helpful discussions.

## References

1. K. F. Liu, *J. Phys. G* **27**, 511 (2001).
2. D. H. Beck and R. D. McKeown, arXiv:hep-ph/0102334 contains an extensive review.
3. R. Hasty *et al.* [SAMPLE Collaboration], *Science* **290**, 2117 (2000).
4. K. A. Aniol *et al.* [HAPPEX Collaboration], *Phys. Lett. B* **509**, 211 (2001).
5. W. Wilcox, *Nucl. Phys. Proc. Suppl.* **94**, 319 (2001).
6. S. J. Dong, K. F. Liu and A. G. Williams, *Phys. Rev. D* **58**, 074504 (1998).
7. N. Mathur and S. J. Dong, *Nucl. Phys. Proc. Suppl.* **94**, 311 (2001).
8. S. J. Dong and K. F. Liu, *Nucl. Phys. Proc. Suppl.* **26**, 353 (1992).
9. S. J. Dong and K. F. Liu, *Phys. Lett. B* **328**, 130 (1994)
10. J. Viehoff *et al.* [SESAM Collaboration], *Nucl. Phys. Proc. Suppl.* **63**, 269 (1998).
11. S. Aoki *et al.* [JLQCD Collaboration], *Nucl. Phys. Proc. Suppl.* **47**, 354 (1996).